Structure and stability of recombinant bovine odorant-binding protein: I. Design and analysis of monomeric mutants

Olga V. Stepanenko[1], Denis O. Roginskii[1], Olesya V. Stepanenko[1], Irina M. Kuznetsova[1], Vladimir N. Uversky[1,3] and Konstantin K. Turoverov[1,2]

[1] Laboratory of Structural Dynamics, Stability and Folding of Proteins, Institute of Cytology, Russian Academy of Science, St. Petersburg, Russia

[2] Peter the Great St. Petersburg Polytechnic University, St. Petersburg, Russia

[3] Department of Molecular Medicine, Morsani College of Medicine, University of South Florida, Tampa, FL, United States

ABSTRACT

Bovine odorant-binding protein (bOBP) differs from other lipocalins by lacking the conserved disulfide bond and for being able to form the domain-swapped dimers. To identify structural features responsible for the formation of the bOBP unique dimeric structure and to understand the role of the domain swapping on maintaining the native structure of the protein, structural properties of the recombinant wild type bOBP and its mutant that cannot dimerize via the domain swapping were analyzed. We also looked at the effect of the disulfide bond by designing a monomeric bOBPs with restored disulfide bond which is conserved in other lipocalins. Finally, to understand which features in the microenvironment of the bOBP tryptophan residues play a role in the defining peculiarities of the intrinsic fluorescence of this protein we designed and investigated single-tryptophan mutants of the monomeric bOBP. Our analysis revealed that the insertion of the glycine after the residue 121 of the bOBP prevents domain swapping and generates a stable monomeric protein bOBP-Gly121+. We also show that the restored disulfide bond in the GCC-bOBP mutant leads to the noticeable stabilization of the monomeric structure. Structural and functional analysis revealed that none of the amino acid substitutions introduced to the bOBP affected functional activity of the protein and that the ligand binding leads to the formation of a more compact and stable state of the recombinant bOBP and its mutant monomeric forms. Finally, analysis of the single-tryptophan mutants of the monomeric bOBP gave us a unique possibility to find peculiarities of the microenvironment of tryptophan residues which were not previously described.

Subjects Biochemistry, Biophysics, Molecular Biology

Keywords Odorant-binding protein, Fluorescence, Protein, Domain swapping, Chemical denaturation, Circular dichroism

Submitted 22 October 2015
Accepted 23 March 2016
Published 18 April 2016

Corresponding authors
Vladimir N. Uversky, vuversky@health.usf.edu
Konstantin K. Turoverov, kkt@incras.ru

Academic editor
Pedro Silva

Additional Information and Declarations can be found on page 21

DOI **10.7717/peerj.1933**

INTRODUCTION

Lipocalins constitute a family of carrier proteins that transport various small hydrophobic molecules ranging from lipids to retinoids, steroids, and bilins. Being found in animals, plants, and bacteria and possessing low sequence identity (less than 20%), these proteins are

characterized by the presence of the conserved "lipocalin fold" that includes two structural modules, an eight-stranded β-barrel that constitutes 70–80% of the protein and includes the ligand-binding site and a C-terminal α-helix with unknown function (*Flower, North & Sansom, 2000*). Evolution of the lipocalin fold generated numerous specialized carrier proteins with the highly diversified binding specificities.

One of the sub-classes of the lipocalin family includes odorant binding proteins (OBPs) with the characteristic ability of reversible binding of various odorant molecules; i.e. volatile, small and hydrophobic compounds with no fixed structure and chemical properties (*Tegoni et al., 2000*). Classic odorant binding protein (OBP) is characterized by a specific monomeric fold, where the eight β-strands, a short α-helical region, and the ninth β-strand interact to form a β-barrel followed by the disordered C-terminal tail (*Bianchet et al., 1996*; *Flower, North & Sansom, 2000*). The ligand binding site of these proteins is formed by hydrophobic and aromatic residues located within the inner cavity of the β-barrel and loop regions connecting β-strands of the barrel. The conserved disulfide bridge formed by Cys 63 and Cys 155 is commonly found in many OBPs to link the flexible C-terminal moiety and strand β4.

Curiously, despite rather high sequence identity between porcine and bovine OBPs (42%), these lipocalins are characterized by different quaternary structures, with porcine OBP (pOBP) being a monomeric protein (*Spinelli et al., 1998*), and with bovine OBP (bOBP) being a dimer (*Bianchet et al., 1996*; *Tegoni et al., 1996*), protomers of which lack the disulfide bridge which is a common feature for all lipocalin family members (*Tegoni et al., 2000*). Therefore, bOBP has a unique dimeric structure, which is quite different from the monomeric folds of the majority of classical OBPs (*Bianchet et al., 1996*; *Stepanenko et al., 2014b*) (Fig. 1). In the bOBP dimer, each of the two protomers forms a β-barrel that interacts with the α-helical portion of the C-terminal tail of other protomer via the domain swapping mechanism. Such a mechanism was described for many dimeric and oligomeric protein complexes, where it plays important structural and functional roles (*Bennett, Schlunegger & Eisenberg, (1995)*; *Van der Wel, (2012)*). It is believed that the increased interaction area between the protein subunits in the complexes formed via the domain swapping mechanism affects the overall protein stability (*Bennett, Choe & Eisenberg, 1994*; *Liu & Eisenberg, 2002*). In some cases, the formation of the quaternary structure of protein by this mechanism is associated with the emergence of new functions in protein oligomers which are not found in the monomeric forms of these proteins (*Liu & Eisenberg, 2002*). Finally, the domain swapping mechanism is involved in the early stages of the amyloid fibril formation (*Van der Wel, 2012*).

In this work, to identify which structural features of bOBP are responsible for the formation of its unique dimeric structure and to understand the role of the domain swapping mechanism in maintaining the native structure of the protein, structural properties of the recombinant wild type bOBP and its four mutant forms that cannot dimerize via the domain swapping (*Ramoni et al., 2008*; *Ramoni et al., 2002*) were analyzed and compared using a spectrum of the biophysical techniques that included intrinsic fluorescence spectroscopy, circular dichroism spectroscopy in the far- and near-UV regions and gel filtration. We also designed two monomeric mutants, GCC-bOBP-W17F and

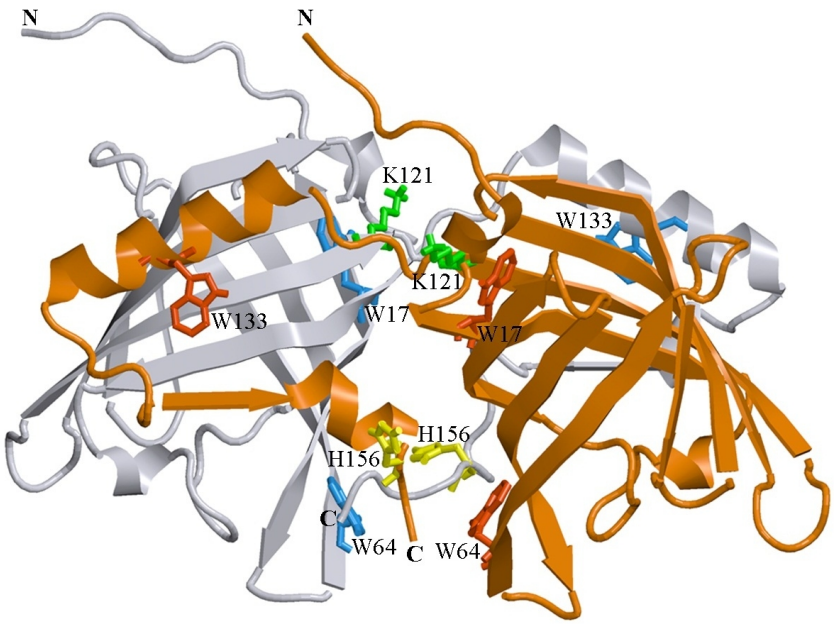

Figure 1 3D structure of bOBP. The individual subunits in the protein are in gray and orange. The tryptophan residues in the different subunits are indicated in red and blue. The Lys 121 residue after which an extra glycine residue are inserted in the mutant form bOBP-Gly121+ is drown in green. Additionally the residues Trp 64 and His 156 (yellow) are substituted for cysteine in the mutant form GCC-bOBP. The drawing was generated based on the 1OBP file (*Tegoni et al., 1996*) from PDB (*Dutta et al., 2009*) using the graphic software VMD (*Hsin et al., 2008*) and Raster3D (*Merritt & Bacon, 1977*).

GCC-bOBP-W133F, each containing a single tryptophan residue, for the characterization of the specific features of the microenvironments of these tryptophan residues that affect the intrinsic fluorescence characteristics of this protein.

MATERIALS AND METHODS

Materials

GdnHCl (Nacalai Tesque, Japan) and 1-octen-3-ol (OCT; Sigma-Aldrich, St. Louis, MO, USA) were used without further purification. The protein concentration was 0.1–0.2 mg/ml. The OCT concentration was 10 mM. The experiments were performed in 20 mM Na-phosphate-buffered solution at pH 7.8.

Gene expression and protein purification

The plasmids pT7-7-bOBP which encodes recombinant bOBP and its mutant forms with a poly-histidine tag were used to transform *Escherichia coli* BL21(DE3) host (Invitrogen) (*Stepanenko et al., 2014b*). The plasmids encoding bOBP and its mutant forms were purchased from Evrogen JSC. Protein expression was induced by incubating the cells with 0.3 mM of isopropyl-beta-D-1-thiogalactopyranoside (IPTG; Fluka, Buchs, Switzerland) for 24 h at 37 °C. The recombinant protein was purified with Ni+-agarose packed in HisGraviTrap columns (GE Healthcare, Uppsala, Sweden). The protein purity was determined through SDS-PAGE in 15% polyacrylamide gel (*Laemmli, 1970*).

Analyzing the 3D protein structure

We analyzed the microenvironment peculiarities for tryptophan residues in the bOBP and GCC-bOBP structure based on PDB data (*Dutta et al., 2009*) using the 1OBP (*Tegoni et al., 1996*) and 2HLV PDB files (*Ramoni et al., 2008*) as described previously (*Giordano et al., 2004*; *Stepanenko et al., 2014a*; *Stepanenko et al., 2015*; *Stepanenko et al., 2012*; *Turoverov, Kuznetsova & Zaitsev, 1985*).

Fluorescence spectroscopy

Fluorescence experiments were performed using a Cary Eclipse spectrofluorometer (Varian, Australia) with microcells FLR (10 × 10 mm; Varian, Australia). Fluorescence intensity was corrected for the primary inner filter effect (*Fonin et al., 2014*). Fluorescence lifetime were measured using a "home built" spectrofluorometer with nanosecond impulse (*Turoverov et al., 1998*) as well as micro-cells (101.016-QS 5 × 5 mm; Hellma, Germany). The decay curves were analyzed using earlier elaborated program (*Turoverov et al., 1998*).

The fitting routine was based on the non-linear least-squares method. Minimization was accomplished according to (*Marquardt, 1963*). P-terphenyl in ethanol and N-acetyl-tryptophanamide in water were used as reference compounds (*Zuker et al., 1985*). Experimental data were analyzed using the multiexponential approach:

$$I(t) = \sum_i \alpha_i \exp(-t/\tau_i)$$

where α_i and τ_i are amplitude and lifetime of component i, respectively, and were $\sum \alpha_i = 1$. At the same time, more physical sense (*Turoverov & Kuznetsova, 1986*) is given by the contribution of i component (with τ_i) S_i to the total emission:

$$S_i = \frac{\alpha_i \int_0^\infty \exp(-t/\tau_i)\,dt}{\sum \alpha_i \int_0^\infty \exp(-t/\tau_i)\,dt} = \frac{\alpha_i \tau_i}{\sum \alpha_i \tau_i}.$$

The root-mean square value of fluorescent lifetimes,$\langle\tau\rangle$, for biexponential decay was determined as

$$\langle\tau\rangle = \frac{\alpha_1 \tau_1^2 + \alpha_2 \tau_2^2}{\alpha_1 \tau_1 + \alpha_2 \tau_2} = \sum S_i \tau_i.$$

Tryptophan fluorescence in the protein was excited at the long-wave absorption spectrum edge ($\lambda_{ex} = 297$ nm), wherein the tyrosine residue contribution to the bulk protein fluorescence is negligible. The fluorescence spectra position and form were characterized using the parameter $A = I_{320}/I_{365}$, wherein I_{320} and I_{365} are the fluorescence intensities at the emission wavelengths 320 and 365 nm, respectively (*Turoverov & Kuznetsova, 2003*). The values for parameter A and the fluorescence spectrum were corrected for instrument sensitivity. The tryptophan fluorescence anisotropy was calculated using the equation:

$$r = (I_V^V - GI_H^V)/(I_V^V + 2GI_H^V),$$

wherein I_V^V and I_H^V are the vertical and horizontal fluorescence intensity components upon excitement by vertically polarized light. G is the relationship between the fluorescence

intensity vertical and horizontal components upon excitement by horizontally polarized light ($G = I_V^H / I_H^H$), $\lambda_{em} = 365$ nm (*Turoverov et al., 1998*).

Protein unfolding was initiated by manually mixing the protein solution (40 μL) with a buffer solution (510 μL) that included the necessary GdnHCl concentration. The GdnHCl concentration was determined by the refraction coefficient using an Abbe refractometer (LOMO, Russia; (*Pace, 1986*)). The dependences of different bOBP fluorescent characteristics on GdnHCl were recorded following protein incubation in a solution with the appropriate denaturant concentration at 4 °C for 2, 24 and 48 h. bOBP refolding was initiated by diluting the pre-denatured protein (in 3.0 M GdnHCl, 40 μL) with the buffer or denaturant solutions at various concentrations (510 μL). The spectrofluorometer was equipped with a thermostat that holds the temperature constant at 23 °C.

Circular dichroism measurements

The CD spectra were generated using a Jasco-810 spectropolarimeter (Jasco, Japan). Far-UV CD spectra were recorded in a 1-mm path length cell from 260 nm to 190 nm with a 0.1 nm step size. Near-UV CD spectra were recorded in a 10-mm path length cell from 320 nm to 250 nm with a 0.1 nm step size. For the spectra, we generated three scans on average. The CD spectra for the appropriate buffer solution were recorded and subtracted from the protein spectra.

Gel filtration experiments

We performed gel filtration experiments for bOBP and its mutant forms in a buffered solution without and with addition of GdnHCl using a Superdex-75 PC 3.2/30 column (GE Healthcare, Sweden) and an AKTApurifier system (GE Healthcare, Uppsala, Sweden). The column was equilibrated with the buffered solution or GdnHCl at the desired concentration, and 10 μl of the protein solution prepared under the same conditions was loaded on the pre-equilibrated column. The change in hydrodynamic dimensions for the studied proteins was evaluated as a change in the bOBP or the mutant protein elution volume. Multiple proteins with known molecular masses (aprotinin (6.5 kDa), ribonuclease (13.7 kDa), carbonic anhydrase (29 kDa), ovalbumin (43 kDa) and conalbumin (75 kDa), which are chromatography standards from GE Healthcare) were used to generate the calibration curve.

Evaluation of the intrinsic disorder predisposition

The intrinsic disorder propensity of the bOBP was evaluated by several disorder predictors, such as PONDR® VLXT (*Dunker et al., 2001*), PONDR® VSL2 (*Peng et al., 2005*), PONDR® VL3 (*Peng et al., 2006*), and PONDR® FIT (*Xue et al., 2010*). Effects of the point mutations on the intrinsic disorder predisposition of this protein was analyzed by PONDR® VSL2. In these analyses, scores above 0.5 are considered to correspond to the disordered residues/regions. PONDR® VSL2B was chosen for the comparative analysis of the bOBP mutants since this tool is one of the more accurate stand-alone disorder predictors (*Fan & Kurgan, 2014*; *Peng & Kurgan, 2012*), PONDR® VLXT is known to have high sensitivity to local sequence peculiarities and can be used for identifying disorder-based interaction sites (*Dunker et al., 2001*), PONDR® VL3 provides accurate evaluation of long disordered

regions (*Peng et al., 2006*), whereas a metapredictor PONDR-FIT is moderately more accurate than each of the component predictors, PONDR® VLXT (*Dunker et al., 2001*), PONDR® VSL2 (*Peng et al., 2005*), PONDR® VL3 (*Peng et al., 2006*), FoldIndex (*Prilusky et al., 2005*), IUPred (*Dosztanyi et al., 2005*), TopIDP (*Campen et al., 2008*). PONDR-FIT (*Xue et al., 2010*).

RESULTS AND DISCUSSION

It is believed that the introduction of an extra glycine residue after the bOBP residue 121 (Fig. 2) should result in the increased mobility of the loop connecting α-helix and 8th β-strand of the β-barrel, which, in its turn, promotes the formation of a monomeric fold of the mutant protein bOBP-Gly121+. Substitutions of the residues Trp64 and His156 to cysteines in bOBP-Gly121+ generate a mutant form GCC-bOBP, which should have stable monomeric structure due to the restoration of the disulfide bond typically seeing in classical OBPs. Finally, to characterize specific features of the microenvironments of tryptophan residues W17 and W133 that might affect the intrinsic fluorescence of the protein, we designed two monomeric mutant forms GCC-bOBP-W17F and GCC-bOBP-W133F, each containing a single tryptophan residue.

To evaluate potential effects of selected mutations on protein structure, we analyzed substitution-induced changes in the intrinsic disorder propensity of bOBP. It has been pointed out that such computational analysis can provide useful information on the expected outcomes of the point mutations in proteins (*Melnik et al., 2012*; *Moroz et al., 2013*; *Uversky et al., 2011*; *Vacic et al., 2012*). Figure 3A represents the results of the computational multi-tool analysis of the per-residue intrinsic disorder predisposition of bOBP. We used here several members of the PONDR family, PONDR® VLXT (*Dunker et al., 2001*), PONDR® VSL2 (*Peng et al., 2005*), PONDR® VL3 (*Peng et al., 2006*), and PONDR-FIT (*Xue et al., 2010*). Figure 3A shows that all these tools are generally agree with each other and indicates that although bOBP is predicted to be mostly ordered, this protein possesses several disordered or flexible regions. Disordered regions are defined here as protein fragments containing residues with the disorder scores above the 0.5 threshold, whereas regions are considered flexible if disorder scores of their residues ranges from 0.3 to 0.5. Figure 3B represents the results of the disorder evaluation in mutant forms of the bOBP and shows the aligned PONDR® VSL2-based disorder profiles for the wild type protein and its four mutants. These analyses revealed that the wild type bOBP and its four mutants are expected to be rather ordered (clearly belonging to the category of hybrid proteins that contain ordered domains and intrinsically disordered regions) and that mutations do not induce significant changes in the bOBP disorder propensity.

Previously, we have shown that the recombinant bOBP, unlike native bOBP purified from the tissue, exists in a stable native-like state as a mixture of monomeric and dimeric forms (*Stepanenko et al., 2014b*) (Table 1). Furthermore, the recombinant bOBP forms dimers in the presence of relatively high denaturant concentrations (e.g., in a solution of 1.5 M guanidine hydrochloride, GdnHCl). The dimerization process is accompanied by the formation of a stable, more compact, intermediate state maximally populated at 0.5M GdnHCl.

1. bOBPwt – wild type protein forms dimer via the domain-swapping mechanism. The protein has 3 tryptophan residues.

```
1          10          20          30          40          50          60
AQEEEAEQNL SELSGPWRTV YIGSTNPEKI QENGPFRTYF RELVFDDEKG TVDFYFSVKR
61         70          80          90          100         110         120
DGKWKNVHVK ATKQDDGTYV ADYEGQNVFK IVSLSRTHLV AHNINVDKHG QTTELTGLFV
121       130         140         150         159
KLNVEDEDLE KFWKLTEDKG IDKKNVVNFL ENEDHPHPE
```

2. bOBP-Gly121+ – the introduction of an extra glycine residue after the bOBP residue 121 is proposed to inhibit dimer formation as a result of the increased mobility of the loop connecting α-helix and 8th β-strand of the β-barrel. The protein contains 3 tryptophan residues as well.

```
1          10          20          30          40          50          60
AQEEEAEQNL SELSGPWRTV YIGSTNPEKI QENGPFRTYF RELVFDDEKG TVDFYFSVKR
61         70          80          90          100         110         120
DGKWKNVHVK ATKQDDGTYV ADYEGQNVFK IVSLSRTHLV AHNINVDKHG QTTELTGLFV
121         130         140         150         159
KGLNVEDEDLE KFWKLTEDKG IDKKNVVNFL ENEDHPHPE
 121+
```

3. GCC- bOBP (bOBP-Gly121+-W64C-H155C) – the substitutions W64C and H155C result in the restoration of the disulfide bond which is necessary for the additional stabilization of the protein. The protein has only 2 tryptophan residues.

```
1          10          20          30          40          50          60
AQEEEAEQNL SELSGPWRTV YIGSTNPEKI QENGPFRTYF RELVFDDEKG TVDFYFSVKR
61         70          80          90          100         110         120
DGKCKNVHVK ATKQDDGTYV ADYEGQNVFK IVSLSRTHLV AHNINVDKHG QTTELTGLFV
121         130         140         150         159
KGLNVEDEDLE KFWKLTEDKG IDKKNVVNFL ENEDCPHPE
 121+
```

4. GCC-bOBP-W17F (bOBP-Gly121+-W64C-H155C-W17F) – the protein contains a single tryptophan residue which allows the investigation of the features of the microenvironment of this residue.

```
1          10          20          30          40          50          60
AQEEEAEQNL SELSGPFRTV YIGSTNPEKI QENGPFRTYF RELVFDDEKG TVDFYFSVKR
61         70          80          90          100         110         120
DGKCKNVHVK ATKQDDGTYV ADYEGQNVFK IVSLSRTHLV AHNINVDKHG QTTELTGLFV
121         130         140         150         159
KGLNVEDEDLE KFWKLTEDKG IDKKNVVNFL ENEDCPHPE
 121+
```

5 GCC-bOBP-W133F (bOBP/Gly121+/W64C/H155C/W133F) – the protein has a single tryptophan residue as well.

```
1          10          20          30          40          50          60
AQEEEAEQNL SELSGPWRTV YIGSTNPEKI QENGPFRTYF RELVFDDEKG TVDFYFSVKR
61         70          80          90          100         110         120
DGKCKNVHVK ATKQDDGTYV ADYEGQNVFK IVSLSRTHLV AHNINVDKHG QTTELTGLFV
121         130         140         150         159
KGLNVEDEDLE KFFKLTEDKG IDKKNVVNFL ENEDCPHPE
 121+
```

Figure 2 **Sequence peculiarities of various bPDB forms.** The comparison of the primary sequence for the recombinant bOBPwt and its mutant forms bOBP-Gly121+ and GCC- bOBP, which are not able to form domain-swapped dimers. The mutant forms GCC-bOBP-W17F and GCC-bOBP-W133F designed to contain a single tryptophan residue were produced to investigate the peculiarities of the microenvironment of the tryptophan residues.

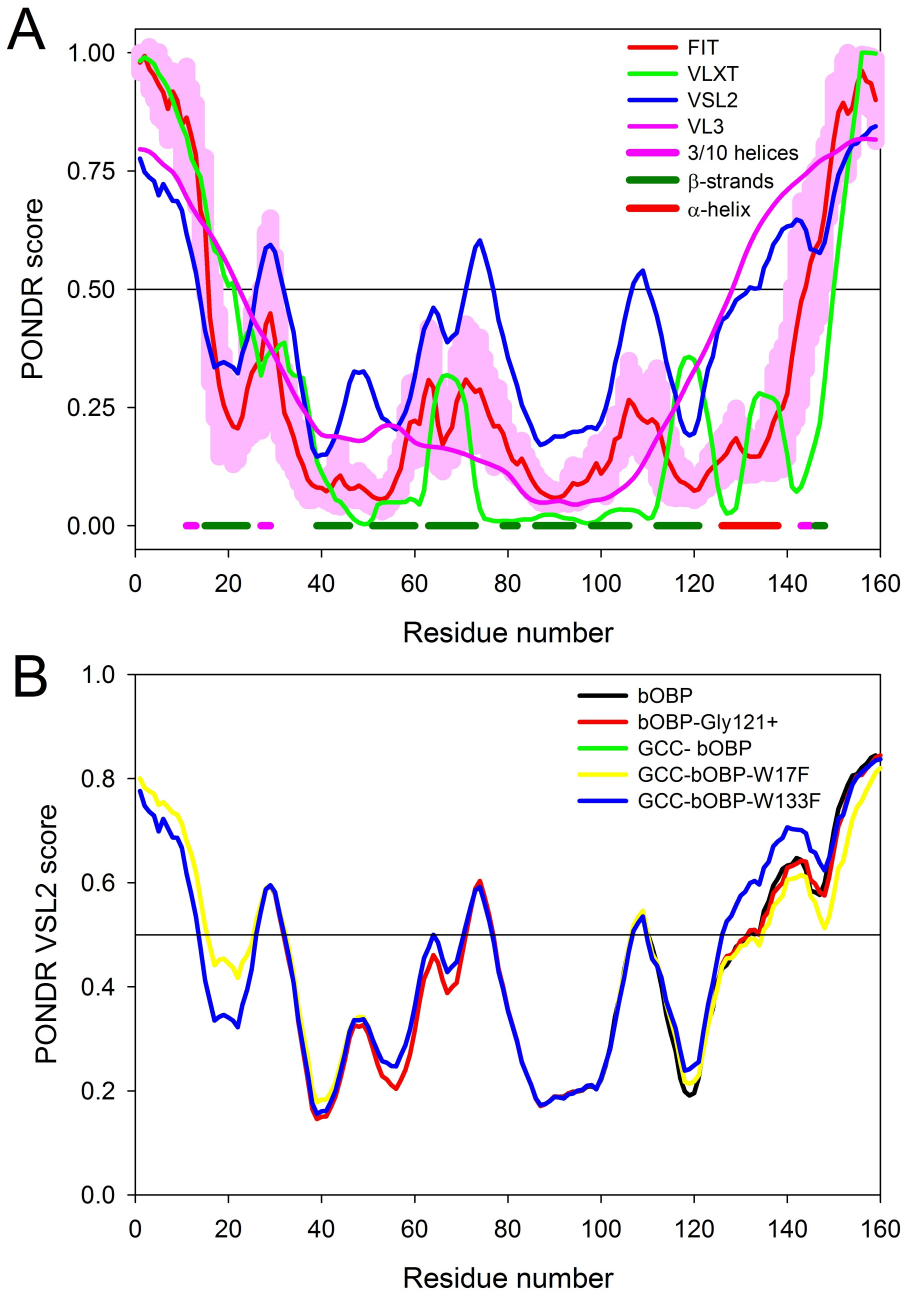

Figure 3 Intrinsic disorder propensity of the wild type bOBP and its mutants. (A) Per-residue disorder propensity of the wild type bOBP evaluated by members of the PONDR family, PONDR® VLXT (*Dunker et al., 2001*) (green line), PONDR® VSL2 (*Peng et al., 2005*) (blue line), PONDR® FIT (*Xue et al., 2010*) (red line) and PONDR® VL3 (*Peng et al., 2006*) (pink line). Localization of known elements of the bOBP secondary structure is shown by colored bars at the bottom of the plot. Light pink shadow around the PONDR® FIT curve represents distribution of errors in the disorder score evaluation. (B) Effects of mutations on the intrinsic disorder propensity of bOBP evaluated by PONDR® VSL2.

Table 1 **Characteristics of recombinant bOBPwt and its mutant forms in different structural states as well as in the presence of natural ligand OCT.**

	Intrinsic fluorescence				Hydrodynamic dimensions	
	λ_{max}, nm[a]	Parameter A[a]	r[b]	$\langle\tau\rangle$, ns:[c] S_i; τ_i (ns)	1 peak, kDa	2 peak, kDa
bOBPwt (*in buffered solution*)[d]	335	1.21	0.170	4.4 ± 0.2: 0.45; 2.7 0.55; 6.0	43.9	23.8
bOBPwt (*in 0.5 M GdnHCl-I_1 state*)[d]	337	1.10	0.166	4.6 ± 0.2: 0.30; 2.6 0.70; 5.3	34.0	19.3
bOBPwt (*in 1.6 M GdnHCl-I_2 state*)[d]	335	1.20	0.180	4.8 ± 0.1: 0.43; 2.5 0.57; 6.4	43.6	
bOBPwt/OCT	334	1.30	0.177		39.6	21.5
bOBPwt in 3.5 M GdnHCl	349	0.47	0.062			
bOBP/Gly121+	336	1.13	0.166	4.6 ± 0.1: 0.14; 1.6 0.86; 5.1	23.6	
bOBP/Gly121+/OCT	335	1.12	0.170		21.5	
bOBP/Gly121+ in 3.5 M GdnHCl	350	0.47	0.059			
GCC-bOBP	335	1.05	0.170	4.3 ± 0.2: 0.45; 2.9 0.55; 5.4	23.6	
GCC-bOBP/OCT	335	1.05	0.174		22.5	
GCC-bOBP in 3.5 M GdnHCl	348	0.48	0.060			
GCC-bOBP-W17F	339	0.82	0.164	4.7 ± 0.1: 0.75; 3.8 0.25; 7.1	23.6	
GCC-bOBP-W17F/OCT	339	0.82	0.165		22.5	
GCC-bOBP-W17F in 3.5 M GdnHCl	349	0.49	0.066			
GCC-bOBP-W133F	325	2.83	0.186	1.9 ± 0.4: 0.73; 0.20 0.27; 4.3	23.6	
GCC-bOBP-W133F/OCT	323	3.02	0.189		23.6	
GCC-bOBP-W133F in 3.5 M GdnHCl	350	0.46	0.056			

Notes.

[a] $\lambda_{ex} = 297$ nm.

[b] $\lambda_{ex} = 297$ nm, $\lambda_{em} = 365$ nm.

[c] $\lambda_{ex} = 297$ nm, $\lambda_{em} = 335$ nm.

[d] The data are from *Stepanenko et al. (2014b)*.

In the present work, gel filtration analysis revealed that all investigated mutants of the bOBP, namely bOBP-Gly121+, GCC-bOBP, GCC-bOBP-W17F, and GCC-bOBP-W133F, are monomers (Fig. 4, Table 1). The positions of the elution peaks of the studied mutant bOBP forms coincided with the position of the elution peak of the monomeric form of recombinant bOBP. This allows us to conclude that monomeric forms of mutant proteins bOBP-Gly121+, GCC-bOBP, GCC-bOBP-W17F, and GCC-bOBP-W133F are as compact

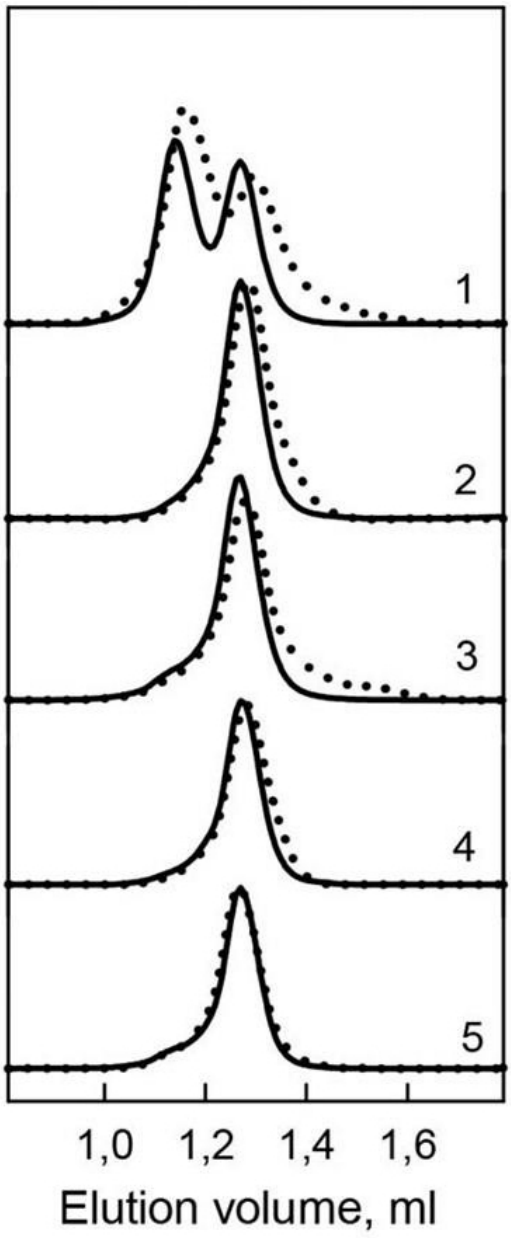

Figure 4 Hydrodynamic characteristics of the bOBP and its mutants. The changes of hydrodynamic dimensions of recombinant bOBP (1) and its mutant forms bOBP-Gly121+ (2), GCC-bOBP (3), GCC-bOBP-W17F (4) and GCC-bOBP-W133F (5) in the absence (solid lines) and the presence of OCT (dotted lines).

as the recombinant bOBP monomer. Therefore, the amino acid substitutions introduced to the bOBP sequence did not affect the compact structure of this protein.

Investigation of the interaction of recombinant bOBP with its natural ligand 1-Octen-3-ol (OCT) by gel-filtration chromatography revealed that the elution profile of the bOBP/OCT complex contained two peaks (Fig. 4). These data indicate that similar to the recombinant bOBP the bOBP/OCT complex exists as a mixture of monomeric and dimeric

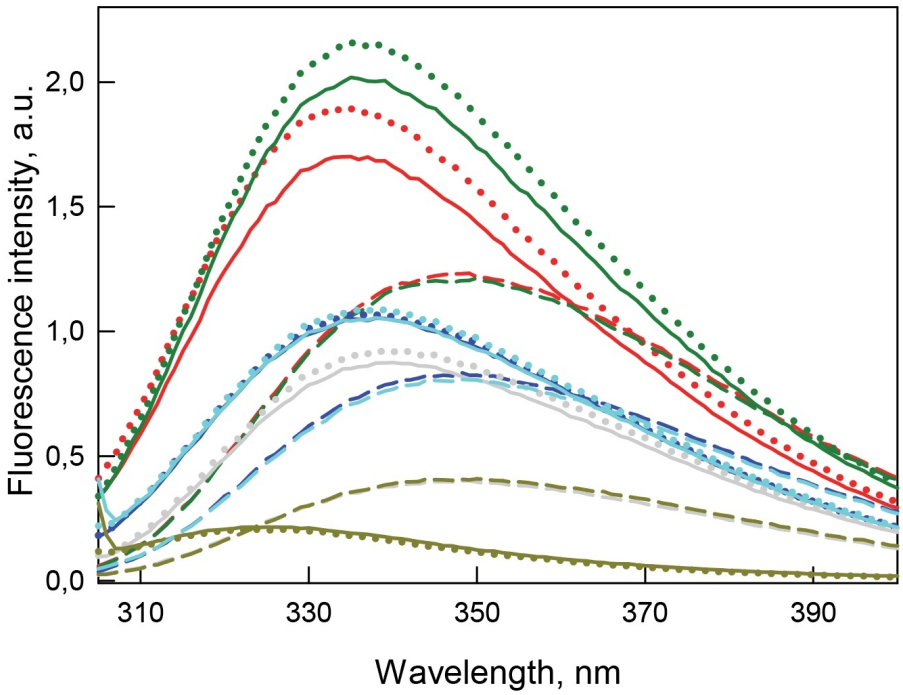

Figure 5 Tertiary structure changes for bOBP (red) and its mutant forms bOBP-Gly121+ (green), GCC-bOBP (blue), GCC-bOBP-W17F (gray) and GCC-bOBP-W133F (dark yellow) in different structural states are indicated by intrinsic tryptophan fluorescence (λ_{ex} = 297 nm). The spectra shown are for the protein in buffered solution (solid line), in the presence of natural ligand OCT (dotted line) and in the presence of 3.5 M GdnHCl (dashed line). The corresponding spectra in light blue were obtained as a sum of the spectra for GCC-bOBP-W17F and GCC-bOBP-W133F.

forms of the protein. However, the positions of the two peaks in the bOBP/OCT elution profile are shifted to slightly higher elution volume, suggesting that the OCT binding induces partial compaction of both the monomeric and dimeric forms of the protein. Evaluated hydrodynamic dimensions of the bOBP and its complex with ligand confirmed this assumption (Table 1). Furthermore, the complexed forms of the bOBP mutants were also more compact than their OCT-free forms (Table 1). The similar behavior of recombinant bOBP and its mutants suggested that the introduced mutations do not affect functional activity of the bOBP and the ability of this protein to bind a natural ligand.

Table 1 and Fig. 5 shows that the recombinant bOBP is characterized by a relatively long-wave position of the intrinsic tryptophan fluorescence (λ_{max} = 335 nm at λ_{ex} = 297 nm). Although in comparison of the position of the emission spectrum of completely solvent accessible Trp (λ_{max} = 350 nm), the indicated value of 335 nm found for the recombinant bOBP is noticeably blue-shifted, this value is definitely too far from a short wavelength position of tryptophan fluorescence found in some proteins. In fact, one of the shortest wavelength position of Trp fluorescence (λ_{max} = 308 nm) was described for the blue copper protein azurine from *Pseudomonas aeruginosa* (*Turoverov, Kuznetsova & Zaitsev, 1985*), and a close short wavelength fluorescence spectra with λ_{max} = 312 nm and 318 nm were also described for the DsbC from *E.coli* (*Stepanenko et al., 2004*) and for another

Table 2 Side chain conformation of Trp residues in bOBPwt and GCC-bOBP.

Protein	Residue	N (*d*)[a]	χ_1, (deg)[a]	χ_2, (deg)[a]
bOBPwt	Trp 17	84 (0.80)	283.18	78.87
	Trp 64	80 (0.71)	278.04	99.85
	Trp 133	56 (0.54)	287.95	112.22
GCC-bOBP	Trp 17	87 (0.83)	292.40	82.09
	Trp 133	48 (0.50)	283.53	103.91

Notes.

[a]N is the number of atoms in the microenvironment of tryptophan residue; *d* is the density of tryptophan residue microenvironment; χ_1 and χ_2 are the angles characterizing the conformation of tryptophan residue side chain.

cooper-containing bacterial protein amicyanin from *Thiobacillus versutus* (*Rosato et al., 1991*), respectively.

The intrinsic fluorescence of bOBP is determined by three tryptophan residues, two of which are located in the β-sheet (Trp17 is in the first β-strand, and Trp64 is in the fourth β-strand), whereas Trp133 is included into a single α-helix of this protein. Among all the tryptophan residues of the protein Trp133 has the lowest density of the microenvironment (d = 0.54), indicating that it is partially accessible to the solvent (Table 2). The microenvironments of Trp17 and Trp64 are more dense (0.80 and 0.71, respectively), but also more polar compared with the Trp133 local environment (Tables 2–5).

It should be noted that the side chains of the charged residues Lys121 and Lys59 included in the microenvironments of Trp17 and Trp64, respectively, are oriented parallel to the indole ring of the corresponding tryptophan residue, and their NZ amino groups are located at a short distance from NE1 group of the corresponding tryptophan residue (5.16 and 4.55 Å for NZ groups Lys121 and Lys59, Tables 3 and 4). Therefore, the presence of a partial fluorescence quenching of Trp17 and Trp64 cannot be excluded, since fluorescence quenching was previously reported for a single tryptophan residue Trp16 of porcine OBP that has similar features in its microenvironment (*Staiano et al., 2007*; *Stepanenko et al., 2008*).

Recombinant bOBP is characterized by high values of fluorescence anisotropy and fluorescence lifetime (Table 1), and also has a pronounced CD spectrum in the near-UV region (Fig. 6). These observations indicate that the environment of tryptophan residues of this protein is quite rigid and asymmetric.

The monomeric bOBP-Gly121+ is characterized by a somewhat longer wavelength of the tryptophan fluorescence spectrum and lower value of the fluorescence anisotropy compared to the recombinant bOBP (Table 1, Fig. 5). The near-UV CD spectrum of the bOBP-Gly121+ is almost indistinguishable for the spectrum of recombinant bOBP (Fig. 6). This indicates that although the overall spatial structure of the protein is not perturbed by adding an extra Gly residue after the position 121, the local microenvironment of the tryptophan residues become less dense due to this sequence perturbation. Importantly, the magnitudes of the fluorescence lifetime and fluorescence quantum yield of the bOBP-Gly121+ are higher than those for the recombinant bOBP. It is likely that the more mobile microenvironments of the tryptophan residues in bOBP-Gly121+ might result in the

Table 3 Characteristics of the Trp 17 microenvironment in bOBPwt and GCC-bOBP.

bOBPwt			GCC-bOBP		
Atoms of the microenvironment	**Atoms of TRP**	**R[a], Å**	**Atoms of microenvironment**	**Atoms of TRP**	**R[a], Å**
Atoms of polar groups					
OG Ser 14	NE1	6.86	Ser 14	NE1	6.61
NE Arg 18	O	4.16	Arg 18	C	6.17
NH1 Arg 18	O	2.95	Arg 18	C	6.46
NH2 Arg 18	O	5.18	OG1 Thr 19	O	6.16
OE1 Glu 42	N	5.44	NH1 Arg 41	O	6.26
OE2 Glu 42	N	6.15	OG Ser 95	CH2	6.02
OG Ser 95	CH2	6.67	OG1 Thr 97	CH2	6.78
ND1 His 98	CZ3	6.87	ND1 His 98	CZ3	6.75
NZ Lys 121	NE1	5.16	NZ Lys 121	NE1	4.83
O HOH 318A	CZ3	6.87	O HOH 1006	O	4.90
			HOH 1047	C	4.33
			HOH 1066	N	5.20
			HOH 1080	CD1	6.62
			HOH 1107	O	6.46
Atoms of peptide bonds					
O Leu 13	NE1	2.87	O Leu 13	NE1	2.74
O Ser 14	NE1	5.05	O Glu 12	NE1	6.62
N Ser 14	NE1	4.86	O Ser 14	NE1	5.11
O Gly 15	N	3.66	N Ser 14	NE1	4.74
N Gly 15	NE1	4.43	O Gly 15	N	3.08
N Pro 16	N	3.54	N Gly 15	CD1	4.19
O Pro 16	N	2.25	N Pro 16	N	3.15
N Arg 18	C	1.32	O Pro 16	N	2.21
O Arg 18	C	3.95	N Arg 18	C	1.33
O Phe 40	O	3.26	O Arg 18	C	3.93
N Phe 40	O	5.10	N Thr 19	C	4.49
N Glu 42	O	4.22	O Thr 19	C	6.91
O Glu 42	CD1	5.73	O Tyr 39	O	6.37
N Leu 43	CD1	4.02	O Phe 40	O	3.24
O Leu 43	CD1	4.49	N Phe 40	O	5.11
O Ser 95	CH2	4.14	N Arg 41	O	3.64
N Ser 95	CH2	5.77	O Arg 41	O	3.53
N Arg 96	CH2	4.71	N Glu 42	O	4.07
O Arg 96	CH2	6.11	O Glu 42	CB	5.54
N Thr 97	CH2	5.09	N Leu 43	CD1	3.86
O Thr 97	CZ3	3.76	O Leu 43	CD1	4.44
O His 98	CH2	4.10	N Val 44	CD1	6.03
N His 98	CZ3	4.14	O Tyr 55	O	5.97
N Leu 99	CZ3	3.74	O Ser 95	CH2	3.55

(*continued on next page*)

Table 3 (*continued*)

bOBPwt			GCC-bOBP		
Atoms of the microenvironment	**Atoms of TRP**	**R[a], Å**	**Atoms of microenvironment**	**Atoms of TRP**	**R[a], Å**
O Leu 99	CZ3	5.57	N Ser 95	CH2	5.32
O Phe 119	CZ3	3.85	N Arg 96	CH2	5.48
N Phe 119	CE3	5.75	O Arg 96	CZ2	4.43
O Val 120	CA	3.38	N Thr 97	CH2	4.59
N Val 120	CE3	3.92	O Thr 97	CZ3	4.10
O Lys 121	CA	6.07	O His 98	CH2	3.67
N Lys 121	CE3	3.51	N His 98	CH2	3.82
N Leu 122	CA	4.61	N Leu 99	CZ3	3.64
O Leu 122	O	5.97	O Leu 99	CZ3	5.59
			N Val 100	CZ3	6.72
			O Phe 119	CZ3	3.53
			N Phe 119	CE3	5.67
			O Val 120	CA	3.51
			N Val 120	CE3	3.73
			O Lys 121	CD2	6.58
			N Lys 121	CE3	3.77
			N Gly 121+	CZ3	6.22
Atoms of nonpolar groups and aromatic residues					
CB Pro 16	N	3.49	CB Pro 16	N	3.73
CB Phe 40	O	3.74	CB Phe 40	O	3.72
CE1 Phe 45	NE1	4.61	CE1 Phe 45	NE1	4.06
CB His 98	CZ3	5.32	CB His 98	CZ3	5.18
CB Phe 119	CE3	4.13	CB Phe 119	CE3	4.08
CD2 Leu 13	CZ2	4.17	CB Leu 13	CZ2	4.65
CB Leu 43	CD1	3.65	CB Leu 43	CD1	3.52
CD1 Leu 94	CH2	4.26	CD1 Leu 94	CH2	4.37
CB Leu 99	CZ3	3.80	CB Leu 99	CZ3	3.75
CB Val 120	CE3	5.51	CB Val 120	CZ3	5.26
CB Lys 121	CD2/CE2	3.83	CD Lys 121	NE1	3.61
CD1 Leu 122	C	4.69			

Notes.

[a]R is the minimal distance between a atom of residue of the microenvironment of tryptophan residue and the nearest atom of its indole ring.

removal of some potential quenching groups from the indole ring of these tryptophan residues, thereby leading to a weakening of the quenching effects.

The values of the fluorescence parameters such as the position of the maximal tryptophan fluorescence, fluorescence anisotropy, and fluorescence lifetime for the triple mutant GCC-bOBP, which was designed to have disulfide bond via substituting residues Trp64 and His156 of the bOBP-Gly121+ to the cysteine residues, were similar to these parameters recorded for the recombinant bOBP (Table 1, Fig. 5). The intensity of the negative band in the near-UV CD spectrum of the GCC-bOBP variant was greater than that of the

Table 4 Characteristics of the Trp 64 microenvironment in bOBPwt.

Atom of the microenvironment	Atom of TRP	R[a], Å
Atoms of polar groups		
OH Tyr 39	CH2	5.35
OG Ser 57	CE3	5.05
NZ Lys 59	NE1	4.55
NZ Lys 63	N	6.58
NZ Lys 65	O	5.23
ND1 His 157	CD1	3.27
NE2 His 157	CD1	4.22
OE1 Glu 159	CH2	5.16
OE2 Glu 159	CH2	4.56
HOH 205A	CH2	4.04
HOH 231A	CZ3	5.70
HOH 247A	CH2	5.80
HOH 282A	CD2	3.74
HOH 289A	CB	4.18
HOH 298A	CZ3	3.56
HOH 328A	NE1	2.88
Atoms of peptide bonds		
N Tyr 39	CZ3	6.04
O Tyr 39	CZ3	6.78
N Ser 57	CZ3	5.96
O Ser 57	CZ3	4.20
N Val 58	CE3/CZ3	4.00
O Val 58	C	3.67
N Lys 59	CE3/CZ3	3.78
O Lys 59	CA	6.52
N Arg 60	N	5.11
O Arg 60	N	5.63
N Lys 63	N	3.61
O Lys 63	N	2.25
N Lys 65	C	1.32
O Lys 65	C	4.07
O Pro 156	CE2	6.63
N His 157	NE1	5.98
O His 157	CZ2	5.90
N Pro 158	CZ2	4.47
O Pro 158	CZ2	6.07
N Glu 159	CZ2	4.12
O Glu 159	NE1	3.31
Atoms of nonpolar groups and aromatic residues		
CE1 Tyr 39	CH2	3.88

(*continued on next page*)

Table 4 (*continued*)

Atom of the microenvironment	Atom of TRP	R[a], Å
CE1 His 155	CE3	6.40
CE1 His 157	CD2	3.52
CD Pro 158	CZ2	3.69
CB Val 58	CZ3	5.50
CB Lys 63	N	3.23
CB Lys 65	C	3.46

Notes.
[a]R is the minimal distance between a residue involved in the microenvironment of tryptophan residue and its indole ring.

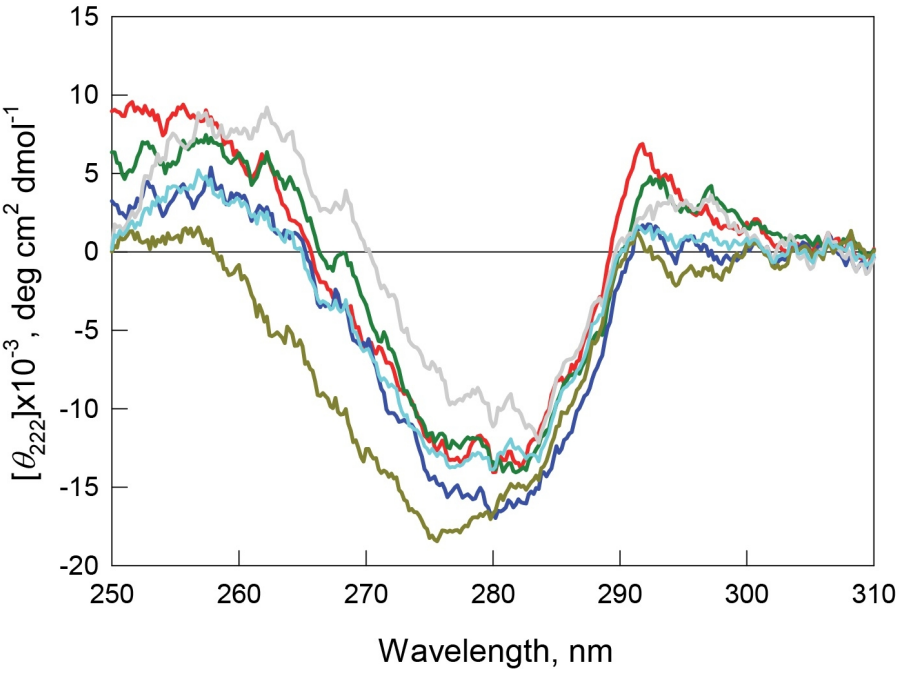

Figure 6 Tertiary structure for bOBP (red) and its mutant forms bOBP-Gly121+ (green), GCC-bOBP (blue), GCC-bOBP-W17F (gray) and GCC-bOBP-W133F (dark yellow) in buffered solution are indicated by near-UV CD spectra. The spectrum in light blue was obtained as a sum of the spectra for GCC-bOBP-W17F and GCC-bOBP-W133F.

recombinant bOBP (Fig. 6). These data demonstrate the stabilizing effect of the disulfide bond to the protein structure. The intensity of the GCC-bOBP tryptophan fluorescence was approximately 25% lower than that of the recombinant bOBP (Fig. 5). Since the structure of the GCC-bOBP retained only two of the three tryptophan residues of the protein, namely Trp17 and Trp133, it can be argued that the removed residue Trp64 made a significant contribution to the fluorescence of recombinant bOBP.

Mutant forms designed to have a single tryptophan residue, GCC-bOBP-W17F (contains only Trp133) and the GCC-bOBP-W133F (contains only Trp17) are characterized by the substantially different parameters of tryptophan fluorescence and near-UV CD spectra (Figs. 5 and 6). GCC-bOBP-W17F has the most long-wavelength fluorescence spectrum

Table 5 Characteristics of the Trp 133 microenvironment in bOBPwt and GCC-bOBP.

bOBPwt			GCC-bOBP		
Atoms of the microenvironment	**Atom of TRP**	**R[a], Å**	**Atoms of the microenvironment**	**Atom of TRP**	**R[a], Å**
Atoms of polar groups					
OH Tyr 21B	CZ2	4.36	OH Tyr 21	NE1	5.03
OG1 Thr 136	CA	4.35	OG1 Thr 136	CA	4.44
NZ Lys 143	CE3	3.35	HOH 1087	CH2	4.99
HOH 218A	CE3/CZ3	4.69			
HOH 2 54A	NE1	3.94			
HOH 232B	NE1	3.27			
HOH 283B	CZ2	5.83			
Atoms of peptide bonds					
N Leu 129	N	6.23	O Leu 129	N	2.97
O Leu 129	N	3.10	O Phe 132	N	2.26
N Glu 130	CD1	4.75	N Lys 134	C	1.33
O Glu 130	N	3.33			
N Phe 132	N	2.85			
O Phe 132	N	2.26			
N Lys 134	C	1.33			
O Lys 134	O	3.28			
N Thr 136	O	3.37			
O Thr 136	O	5.01			
N Lys 143	CZ3	5.56			
O Lys 143	CH2	5.36			
N Val 146	CH2	6.50			
O Val 146	CH2	6.63			
Atoms of nonpolar groups and aromatic residues					
CE2 Tyr 21B	CZ2	4.17	CE2 Tyr 21	NE1	3.96
C Phe 132	N	1.34	C Phe 132	N	1.33
C Leu 129	CD1	3.90	C Leu 129	CD1	4.15
CA Lys 134	C	2.43	CG2Val 146	CZ3	3.98
CG2 Val 146	CZ2	3.69	CA Lys 143	CZ3	4.55
CG Lys 143	CZ3	3.75			

Notes.

[a]R is the minimal distance between a residue involved in the microenvironment of tryptophan residue and its indole ring.

among all proteins studied here, the lowest values of the parameter *A* and the fluorescence anisotropy *r*, whereas GCC-bOBP-W133F has the most short-wavelength fluorescence spectrum and the highest values of the parameter *A* and fluorescence anisotropy *r* (Table 1, Fig. 5). GCC-bOBP-W133F is also characterized by the most intense and short wavelength near-UV CD spectrum. At the same time, the near UV-CD spectrum of the GCC-bOBP-W17F is less intense and the most long wavelength among all proteins analyzed in this study (Fig. 6). These data indicate that the microenvironments of the residues Trp17 and Trp133 are significantly different from each other. It should be noted that the calculated

total spectrum of the intrinsic fluorescence of these two proteins GCC-bOBP-W17F and GCC-bOBP-W133F (calculated as a weighted sum of individual spectra) coincides with the tryptophan fluorescence spectrum of GCC-bOBP (Fig. 5). These data together with the results of the gel filtration analysis suggested that the mutant proteins GCC-bOBP-W17F and GCC-bOBP-W133F maintained native-like, mostly unperturbed spatial structures, and that the microenvironments of their residues Trp17 and Trp133 are similar to the environments of these residues in the GCC-bOBP protein.

The position of the tryptophan fluorescence spectrum of the GCC-bOBP-W17F mutant, and the values of its parameter *A*, fluorescence anisotropy, and fluorescence lifetime suggest that the microenvironment of the Trp133 residue is relatively polar and mobile, and the residue itself contributes significantly to the total fluorescence of this protein (Table 1). These data agree well with the results of the analysis of the specific characteristics of the microenvironment of tryptophan residues in the wild type bOBP (Tables 2–5) and the GCC-bOBP mutant (Tables 2–5). At the same time, the spectral characteristics of the GCC-bOBP-W133F mutant suggest that the Trp17 can be considered as an internal residue located within a very dense, inaccessible to solvent microenvironment. Furthermore, the fluorescence of this residue is substantially quenched (Table 1, Fig. 5).

Analysis of the microenvironment of tryptophan residue Trp17 in the wild type bOBP and its GCC-bOBP mutant (Table 3) shows that it is rather similar to the environment of Trp16 in pOBP, which was considered to be quenched by Lys120 (*Staiano et al., 2007*). However, there are some differences in the conformation of Lys side chain in these proteins. In pOBP, the side chain of Lys120 is located practically parallel to the indole ring of Trp16, and the nearest atom of this residue NZ is separated from the center of the indole ring by only 4.15 Å. This conformation of Lys120 could be stabilized by H-bond formation between the O atom of main chain of Lys15 and NZ atom of Lys120 (2.63 Å, Fig. 7). In bOBP, the side chain of the Lys121 is extended and oriented in such a way that its NZ atom is located far from the center of the indole ring of Trp17. Therefore, it is unlikely that the Trp17 of bOBP is quenched by the Lys121. At the same time, Trp17 of bOBP can be quenched by electron transfer to the amide groups of the main chain. This mechanism works if there are negatively charged groups in the near vicinity of the indole ring and there are positively charged groups near the amides (*Callis, 2014*; *Scott & Callis, 2013*). In the case of Trp17 of bOBP, such situation is provided by Arg18 with its NH1 atom being H-bonded to the amide of the tryptophan residue (2.95 Å) and by Leu13 with its main chain O atom being H-bonded to the indole ring HN (2.87 Å). The Trp64 of bOBP makes a significant contribution to the total fluorescence of the recombinant bOBP. Indeed, in the microenvironment of Trp64 there are no groups which could promote electron transfer to amide groups of the main chain (Table 4). Additionally, the microenvironment of this Trp residue contains only a lysine residue (Lys59) in the conformation similar to that of Lys121, which does not favor fluorescence quenching.

The far-UV CD spectra recorded for the recombinant bOBP and its four mutant forms (bOBP-Gly121+, GCC-bOBP, GCC-bOBP-W17F, and GCC-bOBP-W133F) are rather similar and have a shape characteristic of protein enriched in the β-structural elements (Fig. 8). Decomposition of the far-UV CD spectrum of the recombinant bOBP using the

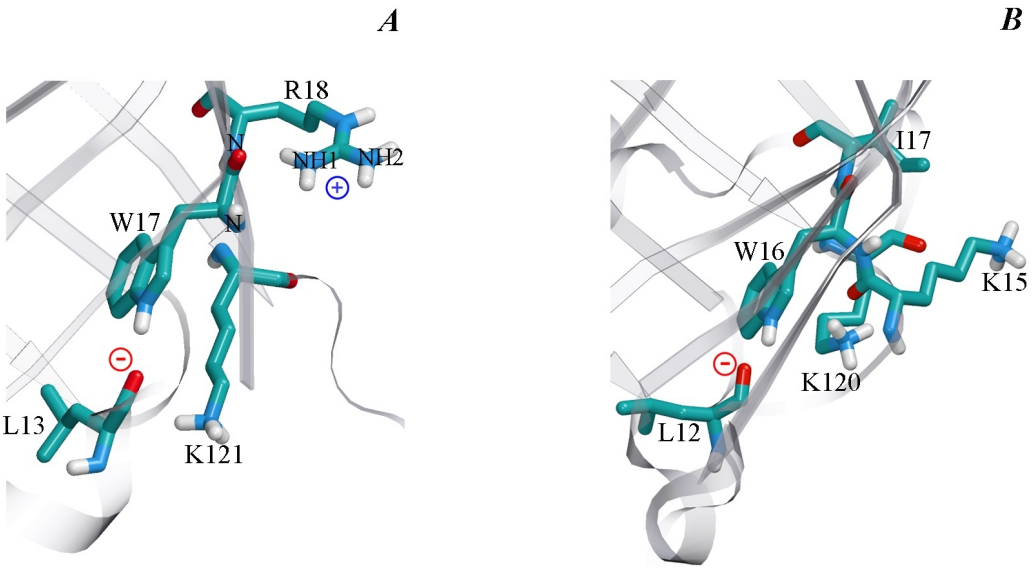

Figure 7 The microenvironment of Trp 17 in bOBP (A) and Trp 16 in pOBP (B). The spatial orientation of lysine residues relative the indole ring of tryptophan residues is shown. The protein core is shown transparent. The drawing was generated based on the 1OBP file (*Tegoni et al., 1996*) and 1A3Y (*Spinelli et al., 1998*) from PDB (*Dutta et al., 2009*) using the graphic software VMD (*Hsin et al., 2008*) and Raster3D (*Merritt & Bacon, 1977*).

Table 6 The evaluation of secondary structure of the recombinant bOBPwt and its mutant forms using Provencher's algorithm (*Provencher & Glockner, 1981*).

	α	β	Turn	Unordered
bOBPwt	0.133	0.359	0.204	0.297
bOBPwt/OCT	0.113	0.354	0.207	0.311
bOBP-Gly121+	0.085	0.400	0.208	0.303
bOBP-Gly121/OCT	0.112	0.407	0.200	0.272
GCC-bOBP	0.134	0.353	0.208	0.293
GCC-bOBP/OCT	0.145	0.344	0.217	0.288
GCC-bOBP W17F	0.077	0.415	0.209	0.299
GCC-bOBP W17F/OCT	0.087	0.429	0.206	0.276
GCC-bOBP W133F	0.154	0.356	0.206	0.269
GCC-bOBP W133F/OCT	0.172	0.352	0.200	0.275

Provencher's algorithm (*Provencher & Glockner, 1981*) revealed that this protein contains 13% α-helix, 36% β-sheet, and 20% β-turns (Table 6). These data agree well with the results of the X-ray analysis of the wild type bOBP (13% α-helix and 46% β-sheets). In the bOBP-Gly121+, adding the Gly121+ insert leads to a certain decrease in the content of α-helical elements (Table 6). Obviously, the insertion of an extra Gly121 residue to the loop segment preceding the single α-helix of the protein reduces the length of this helical element. On the other hand, introduction of a disulfide bond to the structure of the triple mutant GCC-bOBP leads to a full recovery of the protein secondary structure. Since the introduced disulfide bridge tightens the α-helical region to the β-barrel frame of the protein, this tightened overall fold may be the reason for

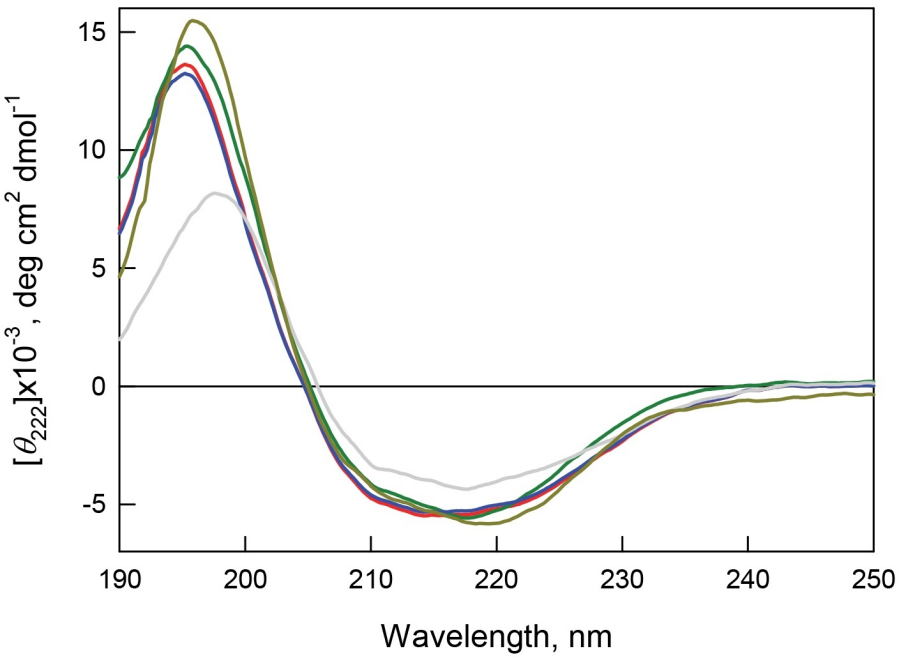

Figure 8 **Secondary structure for bOBP (red) and its mutant forms bOBP-Gly121+ (green), GCC-bOBP (blue), GCC-bOBP-W17F (gray) andGCC-bOBP-W133F (dark yellow) in buffered solution are indicated by far-UV CD spectra.**

the restoration of the bOBP secondary structure. These data also confirm the stabilizing effects of the disulfide bond in the monomeric form of the protein. Replacement of the tryptophan residue Trp133 to phenylalanine in the mutant form GCC-bOBP-W133F leads to an increase in the content of α-helical elements while the content of β-sheets stays unaltered. Instead, the amount of unordered structure is lowered. It is likely that the substitution of the tryptophan residue with a bulky side chain by a less massive residue in the single α-helix of this protein may leads to prolongation of the helical element reducing some steric constraints inside the α-helix. In contrast, in the GCC-bOBP-W17F mutant, replacement of a tryptophan residue Trp17 to phenylalanine may indicate a marked decrease in α-helical structure and marked increase in β-structure with no changes in unordered structure content. We hypothesize that the absence of the bulky side chain of Trp17 in the first β-strand of the β-barrel may favor the formation of a closer contact between the first and the ninth β-strands of the protein thus stabilizing β-barrel.

In the presence of the OCT ligand, the fluorescent characteristics and the near- and far-UV CD spectra of the recombinant bOBP and its mutant forms undergo significant changes, indicating compaction and stabilization of the spatial structure of these proteins (Tables 1 and 6). These data also suggest that all mutant forms of bOBP analyzed in this work retain the ability to bind a natural ligand.

Therefore, all mutant forms of bOBP generally retain tertiary and secondary structure. Their structural organization is rather similar to that of the recombinant bOBP. The structure of the GCC-bOBP is closest to the structure of the recombinant wild type bOBP.

The observed changes in the local structure of the mutant forms of bOBP do not violate the ability of the protein to correctly fold and bind a natural ligand. Ligand binding to the bOBP mutant forms leads to a more compact state of the studied proteins and does not alter its oligomeric status.

CONCLUSIONS

We show here that the insertion of Gly121+ leads to disruption of the domain swapping mechanism, resulting in a stable monomeric mutant protein bOBP-Gly121+. The introduction of a disulfide bond induces noticeable stabilization of the monomeric fold of the GCC-bOBP mutant. The amino acid substitutions introduced to bOBP in this study, such as Gly121+ insertion in the bOBP-Gly121+ mutant, replacement of the Trp64 and His156 to the cysteine residues in the GCC-bOBP mutant, and replacement of the Trp17 and Trp133 residues to phenylalanine in the GCC-bOBP-W17F and GCC-bOBP-W133F mutants, do not disrupt the functional activity of the protein. We show that the ligand binding leads to the formation of a more compact and stable state of the recombinant bOBP and its mutant monomeric forms. We also describe the peculiarities of the microenvironment of tryptophan residues of the protein which are essential for the formation of the fluorescent properties of the protein and which were not described previously.

Abbreviations

bOBP	bovine odorant-binding protein
pOBP	porcine odorant-binding protein
GdnHCl	guanidine hydrochloride
CD	circular dichroism
UV	ultra-violet
Parameter A	(I_{320}/I_{365}) upon excitation at $\lambda_{ex} = 297$ nm

ADDITIONAL INFORMATION AND DECLARATIONS

Funding

This work was supported in part by the Program "Molecular and Cell Biology" of the Russian Academy of Sciences (KKT) and a grant from St. Petersburg in the field of scientific and technological activities (Olga S). The funders had no role in study design, data collection and analysis, decision to publish, or preparation of the manuscript.

Grant Disclosures

The following grant information was disclosed by the authors:
Program "Molecular and Cell Biology" of the Russian Academy of Sciences (KKT).
Grant from St. Petersburg in the field of scientific and technological activities (Olga S).

Competing Interests

Irina M. Kuznetsova, Vladimir N. Uversky and Konstantin K. Turoverov are Academic Editors for PeerJ.

Author Contributions

- Olga V. Stepanenko performed the experiments, analyzed the data, wrote the paper, prepared figures and/or tables, reviewed drafts of the paper.
- Denis O. Roginskii and Olesya V. Stepanenko performed the experiments, analyzed the data, prepared figures and/or tables, reviewed drafts of the paper.
- Irina M. Kuznetsova and Konstantin K. Turoverov conceived and designed the experiments, analyzed the data, wrote the paper, reviewed drafts of the paper.
- Vladimir N. Uversky conceived and designed the experiments, analyzed the data, wrote the paper, prepared figures and/or tables, reviewed drafts of the paper.

Data Availability

The following information was supplied regarding data availability:

All generated data are adequately represented by figures and tables incorporated into the manuscript.

REFERENCES

Bennett MJ, Choe S, Eisenberg D. 1994. Domain swapping: entangling alliances between proteins. *Proceedings of the National Academy of Sciences of the United States of America* **91**:3127–3131 DOI 10.1073/pnas.91.8.3127.

Bennett MJ, Schlunegger MP, Eisenberg D. 1995. 3D domain swapping: a mechanism for oligomer assembly. *Protein Science* **4**:2455–2468 DOI 10.1002/pro.5560041202.

Bianchet MA, Bains G, Pelosi P, Pevsner J, Snyder SH, Monaco HL, Amzel LM. 1996. The three-dimensional structure of bovine odorant binding protein and its mechanism of odor recognition. *Nature Structural Biology* **3**:934–939 DOI 10.1038/nsb1196-934.

Callis PR. 2014. Binding phenomena and fluorescence quenching. II: photophysics of aromatic residues and dependence of fluorescence spectra on protein conformation. *Journal of Molecular Structure* **1077**:22–29 DOI 10.1016/j.molstruc.2014.04.051.

Campen A, Williams RM, Brown CJ, Meng J, Uversky VN, Dunker AK. 2008. TOP-IDP-scale: a new amino acid scale measuring propensity for intrinsic disorder. *Protein & Peptide Letters* **15**:956–963 DOI 10.2174/092986608785849164.

Dosztanyi Z, Csizmok V, Tompa P, Simon I. 2005. IUPred: web server for the prediction of intrinsically unstructured regions of proteins based on estimated energy content. *Bioinformatics* **21**:3433–3434 DOI 10.1093/bioinformatics/bti541.

Dunker AK, Lawson JD, Brown CJ, Williams RM, Romero P, Oh JS, Oldfield CJ, Campen AM, Ratliff CM, Hipps KW, Ausio J, Nissen MS, Reeves R, Kang C, Kissinger CR, Bailey RW, Griswold MD, Chiu W, Garner EC, Obradovic Z. 2001. Intrinsically disordered protein. *Journal of Molecular Graphics and Modelling* **19**:26–59 DOI 10.1016/S1093-3263(00)00138-8.

Dutta S, Burkhardt K, Young J, Swaminathan GJ, Matsuura T, Henrick K, Nakamura H, Berman HM. 2009. Data deposition and annotation at the worldwide protein data bank. *Molecular Biotechnology* **42**:1–13 DOI 10.1007/s12033-008-9127-7.

Fan X, Kurgan L. 2014. Accurate prediction of disorder in protein chains with a comprehensive and empirically designed consensus. *Journal of Biomolecular Structure and Dynamics* **32**:448–464 DOI 10.1080/07391102.2013.775969.

Flower DR, North AC, Sansom CE. 2000. The lipocalin protein family: structural and sequence overview. *Biochimica et Biophysica ACTA* **1482**:9–24.

Fonin AV, Sulatskaya AI, Kuznetsova IM, Turoverov KK. 2014. Fluorescence of dyes in solutions with high absorbance. Inner filter effect correction. *PLoS ONE* **9**:e103878 DOI 10.1371/journal.pone.0103878.

Giordano A, Russo C, Raia CA, Kuznetsova IM, Stepanenko OV, Turoverov KK. 2004. Highly UV-absorbing complex in selenomethionine-substituted alcohol dehydrogenase from Sulfolobus solfataricus. *Journal of Proteome Research* **3**:613–620 DOI 10.1021/pr034132d.

Hsin J, Arkhipov A, Yin Y, Stone JE, Schulten K. 2008. Using VMD: an introductory tutorial. *Current Protocols in Bioinformatics* **Chapter 5**: Unit 5 7 DOI 10.1002/0471250953.bi0507s24.

Laemmli UK. 1970. Cleavage of structural proteins during the assembly of the head of bacteriophage T4. *Nature* **227**:680–685 DOI 10.1038/227680a0.

Liu Y, Eisenberg D. 2002. 3D domain swapping: as domains continue to swap. *Protein Science* **11**:1285–1299 DOI 10.1110/ps.0201402.

Marquardt DW. 1963. An algorithm for least-squares estimation of non-linear parameters. *Journal of the Society for Industrial and Applied Mathematics* **11**:431–441 DOI 10.1137/0111030.

Melnik BS, Povarnitsyna TV, Glukhov AS, Melnik TN, Uversky VN, Sarma RH. 2012. SS-stabilizing proteins rationally: intrinsic disorder-based design of stabilizing disulphide bridges in GFP. *Journal of Biomolecular Structure and Dynamics* **29**:815–824 DOI 10.1080/07391102.2012.10507414.

Merritt EA, Bacon DJ. 1977. Raster3D: photorealistic molecular graphics. *Methods in Enzymology* **277**:505–524.

Moroz NA, Novak SM, Azevedo R, Colpan M, Uversky VN, Gregorio CC, Kostyukova AS. 2013. Alteration of tropomyosin-binding properties of tropomodulin-1 affects its capping ability and localization in skeletal myocytes. *Journal of Biological Chemistry* **288**:4899–4907 DOI 10.1074/jbc.M112.434522.

Pace CN. 1986. Determination and analysis of urea and guanidine hydrochloride denaturation curves. *Methods in Enzymology* **131**:266–280 DOI 10.1016/0076-6879(86)31045-0.

Peng ZL, Kurgan L. 2012. Comprehensive comparative assessment of in-silico predictors of disordered regions. *Current Protein & Peptide Science* **13**:6–18 DOI 10.2174/138920312799277938.

Peng K, Radivojac P, Vucetic S, Dunker AK, Obradovic Z. 2006. Length-dependent prediction of protein intrinsic disorder. *BMC Bioinformatics* **7**:208 DOI 10.1186/1471-2105-7-208.

Peng K, Vucetic S, Radivojac P, Brown CJ, Dunker AK, Obradovic Z. 2005. Optimizing long intrinsic disorder predictors with protein evolutionary information. *Journal of Bioinformatics and Computational Biology* **3**:35–60 DOI 10.1142/S0219720005000886.

Prilusky J, Felder CE, Zeev-Ben-Mordehai T, Rydberg EH, Man O, Beckmann JS, Silman I, Sussman JL. 2005. FoldIndex: a simple tool to predict whether a given protein sequence is intrinsically unfolded. *Bioinformatics* **21**:3435–3438 DOI 10.1093/bioinformatics/bti537.

Provencher SW, Glockner J. 1981. Estimation of globular protein secondary structure from circular dichroism. *Biochemistry* **20**:33–37 DOI 10.1021/bi00504a006.

Ramoni R, Spinelli S, Grolli S, Conti V, Merli E, Cambillau C, Tegoni M. 2008. Deswapping bovine odorant binding protein. *Biochimica et Biophysica ACTA* **1784**:651–657 DOI 10.1016/j.bbapap.2008.01.010.

Ramoni R, Vincent F, Ashcroft AE, Accornero P, Grolli S, Valencia C, Tegoni M, Cambillau C. 2002. Control of domain swapping in bovine odorant-binding protein. *Biochemical Journal* **365**:739–748 DOI 10.1042/bj20011631.

Rosato N, Mei G, Savini I, Del Bolgia F, Finazzi-Agro A, Lommen A, Canters GW. 1991. Intrinsic fluorescence of the bacterial copper-containing protein amicyanin. *Archives of Biochemistry and Biophysics* **284**:112–115 DOI 10.1016/0003-9861(91)90271-J.

Scott JN, Callis PR. 2013. Insensitivity of tryptophan fluorescence to local charge mutations. *The Journal of Physical Chemistry B* **117**:9598–9605 DOI 10.1021/jp4041716.

Spinelli S, Ramoni R, Grolli S, Bonicel J, Cambillau C, Tegoni M. 1998. The structure of the monomeric porcine odorant binding protein sheds light on the domain swapping mechanism. *Biochemistry* **37**:7913–7918 DOI 10.1021/bi980179e.

Staiano M, D'Auria S, Varriale A, Rossi M, Marabotti A, Fini C, Stepanenko OV, Kuznetsova IM, Turoverov KK. 2007. Stability and dynamics of the porcine odorant-binding protein. *Biochemistry* **46**:11120–11127 DOI 10.1021/bi7008129.

Stepanenko OV, Bublikov GS, Stepanenko OV, Shcherbakova DM, Verkhusha VV, Turoverov KK, Kuznetsova IM. 2014a. A knot in the protein structure—probing the near-infrared fluorescent protein iRFP designed from a bacterial phytochrome. *FEBS Journal* **281**:2284–2298 DOI 10.1111/febs.12781.

Stepanenko OV, Fonin AV, Stepanenko OV, Staiano M, D'Auria S, Kuznetsova IM, Turoverov KK. 2015. Tryptophan residue of the D-galactose/D-glucose-binding protein from *E. Coli* localized in its active center does not contribute to the change in intrinsic fluorescence upon glucose binding. *Journal of Fluorescence* **25**:87–94 DOI 10.1007/s10895-014-1483-z.

Stepanenko OV, Kuznetsova IM, Turoverov KK, Huang C, Wang CC. 2004. Conformational change of the dimeric DsbC molecule induced by GdnHCl. A study by intrinsic fluorescence. *Biochemistry* **43**:5296–5303 DOI 10.1021/bi0359325.

Stepanenko OV, Marabotti A, Kuznetsova IM, Turoverov KK, Fini C, Varriale A, Staiano M, Rossi M, D'Auria S. 2008. Hydrophobic interactions and ionic networks play an important role in thermal stability and denaturation mechanism of the porcine odorant-binding protein. *Proteins* **71**:35–44 DOI 10.1002/prot.21658.

Stepanenko OV, Stepanenko OV, Kuznetsova IM, Shcherbakova DM, Verkhusha VV, Turoverov KK. 2012. Distinct effects of guanidine thiocyanate on the structure of superfolder GFP. *PLoS ONE* **7**:e48809 DOI 10.1371/journal.pone.0048809.

Stepanenko OV, Stepanenko OV, Staiano M, Kuznetsova IM, Turoverov KK, D'Auria S. 2014b. The quaternary structure of the recombinant bovine odorant-binding protein is modulated by chemical denaturants. *PLoS ONE* **9**:e85169 DOI 10.1371/journal.pone.0085169.

Tegoni M, Pelosi P, Vincent F, Spinelli S, Campanacci V, Grolli S, Ramoni R, Cambillau C. 2000. Mammalian odorant binding proteins. *Biochimica et Biophysica ACTA* **1482**:229–240 DOI 10.1016/S0167-4838(00)00167-9.

Tegoni M, Ramoni R, Bignetti E, Spinelli S, Cambillau C. 1996. Domain swapping creates a third putative combining site in bovine odorant binding protein dimer. *Nature Structural Biology* **3**:863–867 DOI 10.1038/nsb1096-863.

Turoverov KK, Biktashev AG, Dorofeiuk AV, Kuznetsova IM. 1998. A complex of apparatus and programs for the measurement of spectral, polarization and kinetic characteristics of fluorescence in solution. *Tsitologiia* **40**:806–817.

Turoverov KK, Kuznetsova IM. 1986. What causes the variation of polarization degree across the emission spectrum of proteins? *Biophysical Chemistry* **24**:327–335 DOI 10.1016/0301-4622(86)85038-4.

Turoverov KK, Kuznetsova IM. 2003. Intrinsic fluorescence of actin. *Journal of Fluorescence* **13**:41–57 DOI 10.1023/A:1022366816812.

Turoverov KK, Kuznetsova IM, Zaitsev VN. 1985. The environment of the tryptophan residue in Pseudomonas aeruginosa azurin and its fluorescence properties. *Biophysical Chemistry* **23**:79–89 DOI 10.1016/0301-4622(85)80066-1.

Uversky VN, Shah SP, Gritsyna Y, Hitchcock-DeGregori SE, Kostyukova AS. 2011. Systematic analysis of tropomodulin/tropomyosin interactions uncovers fine-tuned binding specificity of intrinsically disordered proteins. *Journal of Molecular Recognition* **24**:647–655 DOI 10.1002/jmr.1093.

Vacic V, Markwick PR, Oldfield CJ, Zhao X, Haynes C, Uversky VN, Iakoucheva LM. 2012. Disease-associated mutations disrupt functionally important regions of intrinsic protein disorder. *PLoS Computational Biology* **8**:e1002709 DOI 10.1371/journal.pcbi.1002709.

Van der Wel PC. 2012. Domain swapping and amyloid fibril conformation. *Prion* **6**:211–216 DOI 10.4161/pri.18987.

Xue B, Dunbrack RL, Williams RW, Dunker AK, Uversky VN. 2010. PONDR-FIT: a meta-predictor of intrinsically disordered amino acids. *Biochimica et Biophysica ACTA* **1804**:996–1010 DOI 10.1016/j.bbapap.2010.01.011.

Zuker M, Szabo AG, Bramall L, Krajcarski DT, Selinger B. 1985. The delta function convolution method (DFCM) for fluorescence decay experiments. *Review of Scientific Instruments* **56**:14–22 DOI 10.1063/1.1138457.